Journal of Photochemistry and Photobiology A: Chemistry 216 (2010) 142–148

Contents lists available at ScienceDirect

Journal of Photochemistry and Photobiology A: Chemistry

journal homepage: www.elsevier.com/locate/jphotochem

# Sol–gel nanoparticulate mesoporous films with enhanced self-cleaning properties

Morgan Gohin[a], Emmanuelle Allain[a], Nicolas Chemin[b], Isabelle Maurin[a], Thierry Gacoin[a,*], Jean-Pierre Boilot[a]

[a] Groupe de Chimie du Solide, Laboratoire de Physique de la Matière Condensée, CNRS-Ecole Polytechnique, UMR 7643, 91128 Palaiseau, France
[b] Saint-Gobain Recherche, 39 Quai Lucien Lefranc, 93303 Aubervilliers, France

ARTICLE INFO

*Article history:*
Available online 3 July 2010

*Keywords:*
Self-cleaning
Photocatalysis
Sol–gel coatings
Mesoporous silica
N-doped $TiO_2$

ABSTRACT

This paper presents a brief overview of the work done in our group concerning a versatile approach for the elaboration of $TiO_2$-based photocatalytic coatings through the use of preformed $TiO_2$ colloidal particles dispersed within a surfactant-templated mesoporous silica binder. Investigation of the influence of porosity on the photocatalytic efficiency of these films showed that the major impact arises from diffusion of the pollutant molecules (stearic acid) within the volume of the film, thus improving the action of the radicals photogenerated at the surface of the $TiO_2$ particles. Starting from standard films elaborated using a commercial colloid, we showed that our approach allows a systematic investigation of any systems available as a colloidal suspension. A first example is given on titanium dioxide nanopowders (calcined Millennium or Degussa P25 particles). A grinding process was developed allowing the recovery of these powders as suspension of 120 nm aggregates that can be subsequently incorporated within mesoporous silica films. The obtained films exhibited photocatalytic performances similar to those of the standard films directly synthesized with the Millennium colloid. This result implies that the influence of the microstructure on photocatalytic efficiency is mainly governed by the silica matrix, allowing the investigation of almost any compounds even those synthesized through conventional solid state reaction at high temperature. We also developed an original process to prepare colloidal solutions of N-doped $TiO_2$ particles obtained by nitridation treatment at high temperature. Investigation of the doping and photocatalytic efficiency under visible light irradiation evidenced the competition between nitrogen insertion and detrimental $Ti^{4+}$ reduction. The latter effect may be somewhat limited by a post-treatment under air that re-oxidize the $Ti^{3+}$ while preserving part of the inserted nitrogen.



## 1. Introduction

Titanium dioxide is well known for its exceptional photocatalytic properties leading to innovative applications [1]. Self-cleaning materials are based on the photo-degradation of organic pollutants nearby the surface of a substrate onto which a $TiO_2$ film has been deposited. Such $TiO_2$ films may be deposited using different techniques such as sputtering [2], chemical vapor deposition (CVD) [3] or sol–gel process [4]. Although leading to films with a lower durability, the sol–gel chemistry allows the best control of the microstructure of the films, especially their porosity and specific surface area which are known to have a drastic influence on the photocatalytic efficiency [5,6]. One method to control the porosity of sol–gel films is to use surfactant micellar templates [7]. This strategy has been successfully studied in the case of photocatalytic silica/$TiO_2$ composite films in our group and many others [8–10]. In our case, we focused our attention on a method that relies on the incorporation of preformed colloidal $TiO_2$ particles within a mesoporous silica binder [10].

Starting from this seminal work, we discuss here on the influence of the film porosity that can be finely tuned in our process by varying the surfactant/silica molar ratio. Results are discussed in relation with the degradation process that is proposed in the specific case of these films. The second part of this paper focuses on the use of preformed $TiO_2$ particles that allows a modulation of the structure, size and shape of these particles without modifying the overall microstructure of the film that is mainly governed by the mesoporous silica host matrix. Results are reported on different particles, among which commercial 50 nm Millennium particles and P25 Degussa particles obtained after an original grinding/dispersion process starting from the commercial nanopowder. Finally, we present recent results concerning the sensitization our films toward visible light using N-doped $TiO_2$. This study was performed through a process allowing the synthesis of well dis-

* Corresponding author. Tel.: +33 1 6933 4656; fax: +33 1 6933 4799.
*E-mail address:* thierry.gacoin@polytechnique.fr (T. Gacoin).

1010-6030/$ – see front matter © 2010 Elsevier B.V. All rights reserved.
doi:10.1016/j.jphotochem.2010.06.029

persed colloidal particles that were first submitted to a nitridation treatment at high temperature. Results are discussed in term of competition between the sensitization effects due to nitrogen insertion and the concomitant reduction of $Ti^{4+}$ that drastically alters the film activity.

## 2. Experimental

### 2.1. Elaboration of colloidal $TiO_2$-based films

The elaboration of the $TiO_2/SiO_2$ nanocomposite films was fully described in a previous paper [10]. In a first step, a silica sol was prepared by hydrolysis and aging of tetraethoxysilane (TEOS) under acidic conditions. The copolymer (PE6800, BASF) was then dissolved into the obtained sol, with the appropriate quantity depending on the copolymer/silica molar ratio (hereafter noted Copo/Si). In "standard" films, the Copo/Si ratio was taken equal to 0.01. The $TiO_2$ particles were then mixed to the obtained sol by slowly adding a given volume of an aqueous $TiO_2$. The relative molar ratio of $TiO_2$ compared to $SiO_2 + TiO_2$ is hereafter noted Ti/(Ti + Si). This ratio was usually taken equal to 0.5. The substrate is common float glass onto which was deposited a very thin sodium diffusion barrier of $SiO_2$. Just after deposition, the films were dried and calcined under air at 450 °C for 1.5 h to remove the surfactant. Standard films have a typical thickness of 400 nm.

### 2.2. Elaboration of colloidal suspensions from oxide nanopowders

Grinding experiments were performed in air with a planetary ball mill (Fritsch Pulverisette 6). A 80 ml zirconia vial was used with 10 zirconia balls (15 mm in diameter). Ball milling was carried out on a mixture containing 1 g of the oxide powder (e.g. Degussa P25), 10 g of ZnO (10 g, 99% Fluka) and 25 ml of diethyleneglycol. The mixture to ball volume ratio was approximately 1/1. The grinding conditions consisted of 10 cycles of 15 min each at 500 rpm, spaced by 6 min to minimize heating effects. At this rotation speed, the process involved both homogenization and grinding of the mixture through frictional and impact forces. The recovered suspension was then treated with acetic acid to dissolve the ZnO matrix and extensively washed with water. The particles were finally dispersed in a HCl solution at pH 1.25 with a concentration of ca. 150 g $L^{-1}$. Photocatalytic films were synthesized incorporating the suspension as previously described in the case of the commercial Millennium colloid.

### 2.3. Nitridation process for the colloidal $TiO_2$ particles [11,12]

$TiO_2$ colloids were first embedded in mesoporous silica powder, following a process similar to the one described above, using a Ti/(Ti + Si) molar ratio of 1/3. The sol was not spin-coated but dried until getting a powder which was heated at 450 °C for 30 h to remove the surfactant. 1 g of this $TiO_2/SiO_2$ nanocomposite powder was inserted in a tubular furnace with 3 g of urea. After Argon flush during 2 h, the powder was heated at different temperatures ranging from 500 to 800 °C for 2 h under neutral atmosphere. After the thermal treatment, the silica matrix was totally dissolved by hydrofluoric acid treatment during 2 h (HF, 2 wt% in water). The obtained solution was centrifuged and rinsed with distilled water at least three times, and then dispersed into an aqueous acidic solution of HCl with pH 1.25. This colloidal solution was then used to prepare mesoporous silica films containing N-doped $TiO_2$ NPs, using the procedure described above. The $TiO_2$ amount per surface unit on these N-doped films was 4.6 μg $cm^{-2}$.

## 3. Results and discussion

### 3.1. Microstructure of the $TiO_2/SiO_2$ nanoparticulate films and influence of the porosity on photocatalytic efficiency

Fig. 1 shows a typical TEM image of a transverse section of a film containing the Millennium particles as shown in insert. The particles are clearly well dispersed all over the film thickness (ca. 400 nm). White dots correspond to the mesopores of the silica binder which size is about 3–5 nm. Fig. 1 (right) gives a schematic description of the porosity in such films as determined by porosimetry. In addition to the mesopores, there is a microporosity (pore size less than 2 nm) which results from to the limited condensation of the silica walls. The global volume fractions of mesopores and micropores within a standard film are 39% and 9% respectively, while the overall surface area is about 450 $m^2$ $g^{-1}$ [10].

Detailed investigation of the degradation kinetics on these films showed a first order rate over all a degradation experiment, but with a $k_1$ constant that was found to be inversely proportional to the initial amount of pollutant (stearic acid) deposited on the film [10]. Characterization of the localization of the molecules before their degradation was achieved by considering the carbon profile as deduced from SIMS analysis. It can be shown that using a 10 g $L^{-1}$ solution of stearic acid, molecules were completely absorbed by the film porosity for pore volume fraction larger than 8%. In this case, as schematically shown in Fig. 2 (right), all the molecules are adsorbed within the film thickness and the degradation proceeds through the diffusion of photogenerated radicals from the surface of the $TiO_2$ particles [13]. We infer, from preliminary numerical simulation of the degradation process, that the complex kinetics behaviour of our film may be explained by the process shown in Fig. 2 (bottom right), involving a progressive depletion of pollutant molecules from the surface of the $TiO_2$ particles.

Fig. 2 (left) shows the evolution of the $k_1$ constant as a function of the film porosity which was varied by changing the relative amount of the copolymer template as compared to the silica fraction (the standard film corresponds to Copo/Si = 0.01 leading to a porosity of 48%). The curve evidences a linear increase of the activity until reaching a maximum for porosity values larger than ca. 30%. It may be inferred that the efficiency of the degradation depends on the average distance between the pollutant molecules and the surface of the $TiO_2$ particles where the radicals are generated. This explains the initial increase observed when crossing the point where part of the molecules are located at the surface of the film as compared to the case where the molecules are only dispersed within the film thickness (threshold value at 10% porosity, see Fig. 2 (left)). Considering that, for porosity values larger than 10%, the average distance between the molecules and the particles is not changed, the continuous increase of the degradation rate as a function of the porosity reveals the influence of the silica matrix. This beneficial effect is limited to the adsorption of a complete monolayer of pollutant molecules on the silica walls, explaining the saturation for porosity larger than 30%.

### 3.2. Application of the process for the study of other colloidal particles

As previously mentioned, a decisive advantage of the process is the ability to synthesize films starting for almost any available colloidal suspension of photo-active compounds [10,14]. This allows studying the influence of the particles themselves without changing the overall microstructure of the film, which remains mainly governed by the mesoporous silica host binder. Thus, one can study the influence of size, crystalline structure and chemical composition of the particles provided that the compounds can be obtained as dispersions of NPs with a sufficient concentration.

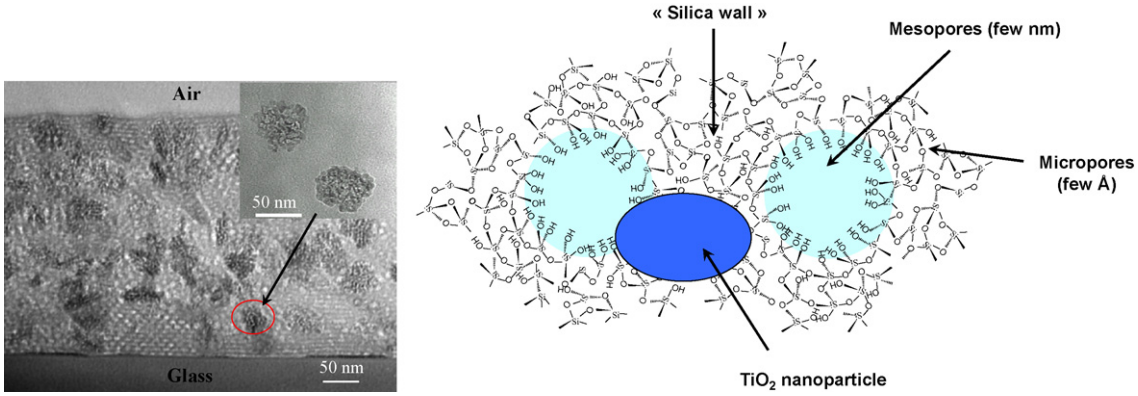


**Fig. 1.** Typical TEM image of a transverse section of a film containing Millennium $TiO_2$ NPs (left) and schematic representation the film porosity (right).

Colloidal suspensions are generally obtained through colloid chemistry that relies on reactions of precipitation from precursors in solution. When optimized, this strategy allows a good control of the size and dispersion state of NPs. However, this approach is time consuming and should only be considered in the case of systems that have already proven their efficiency. Moreover, the moderate temperatures that are involved in the synthesis process limit this strategy to systems like $TiO_2$ that can be obtained in good crystalline state under these conditions.

In this context, it appeared as interesting to develop a grinding process that would allow studying compounds that are obtained by solid state reactions at high temperature, i.e. which colloidal synthesis is not yet reported. In the context of developing new systems active under visible light irradiation, large amount of work have been done to seek for other compositions than pure $TiO_2$. This could be achieved by doping of $TiO_2$, designing heterostructures that couple $TiO_2$ to another semiconductor or looking for different compounds. For example, $BaM_{1/3}N_{2/3}O_3$ (M = Ni, Zn, N = Nb, Ta) [15], compounds of wolframite structure as $In_{0.8}M_{0.2}TaO_4$ (M = Mn, Fe, Co, Ni, Cu) [16] have been proposed. Other studies have shown the interest of bismuth phases like $Bi_{12}GeO_{20}$ [17], $Bi_{12}TiO_{20}$ and of heterostructures based on indium $InVO_4/TiO_2$ [18] or iron $Fe_2O_3/SrTiO_3$ [19] oxides. In most cases, these materials were synthesized by solid state reaction routes, which require heat treatment at high temperatures leading to agglomerated powders. The potential applications of these materials were then mostly restricted to air and water purification, or water splitting.

Starting from the results obtained for micronic powders, and considering the targeted application of self-cleaning transparent coatings, it is necessary to prepare the photocatalytic material as a colloidal suspension. Instead of developing a time consuming colloidal synthesis of these compounds, we decided to investigate a method that would allow, starting from powders obtained by solid state reactions at high temperature, to recover particles as suspensions after grinding. In this case, if a good control of the particle size is difficult, the technique is relatively simple to implement, with the insurance to preserve particle composition and structural phase at least for rather low-energy grinding.

The first step of this preparation is thus to reduce the material to a fine powder by grinding using a planetary ball mill [20–22] and further disperse the particles in a solvent compatible with the silica sol–gel synthesis. One drawback often observed after milling is that the ground particles tend to form aggregates relatively dispersed in size. To circumvent this problem, we have developed an original method that consists in milling in presence of a large amount of ZnO (Fig. 3). This approach presents several advantages: (i) improvement the grinding efficiency by friction; (ii) reduction of the aggregation between particles by matrix effect; (iii) the high solubility of ZnO in acidic media allows an easy dispersion of the ground particles in solution.

Diethyleneglycol, a polar solvent with a high boiling point (245 °C), was also added in the ball mill to improve the grinding efficiency and also to prevent a large agglomeration of the particles. After grinding, dissolution of the ZnO matrix, and transfer of the particles into acidic water, the as-obtained suspensions were recovered with a concentration of 150 g $L^{-1}$. These solutions were then used to deposit $SiO_2$–$TiO_2$ nanocomposite films as previously described.

One of the main issues is to ensure that the measured photocatalytic activity merely reflects that of the sample and is not

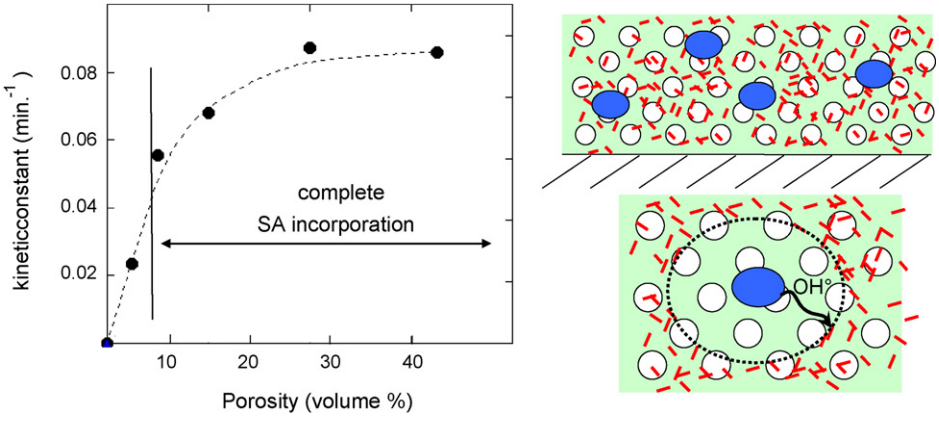


**Fig. 2.** Evolution of the kinetic constant, $k_1$ as a function of the film porosity (left), and schematic representation of the stearic acid (SA) localization before and during the degradation process (right).

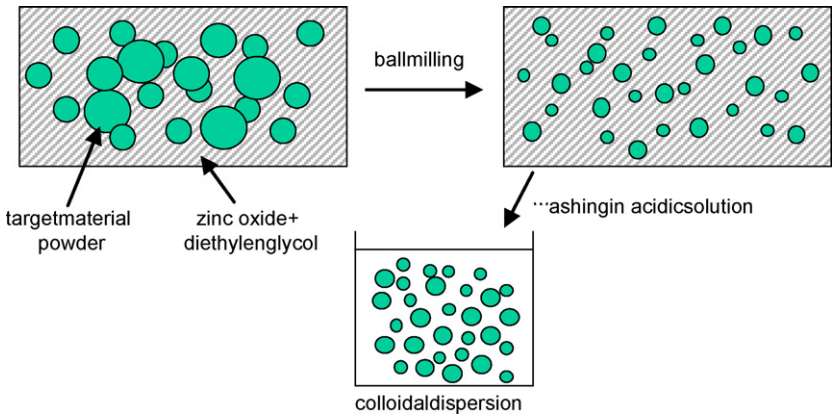


**Fig. 3.** Schematic protocol of the grinding experiments. The powder is first mixed with zinc oxide in diethyleneglycol before being crushed in a planetary ball. Zinc oxide is then removed by washing in an acidic aqueous solution and finally dispersed in a pH 1.25 solution.

associated to parasitic effects such as contamination by Zn traces, particle size reduction, increased light scattering in the layer, or partial structural transition to the rutile phase during grinding for $TiO_2$-based materials [23]. To validate our approach, we first compared the photocatalytic activity under UV light of two films, with a same $TiO_2$ loading, prepared either directly using the commercial Millennium $TiO_2$ colloid (diluted to 150 g $L^{-1}$), or from the same NPs dried at 90 °C, heated up to 450 °C in air for 2 h to form agglomerates. This latter sample was further ground by ball milling following the previous protocol. In this experiment, it is mostly the aggregation state of particles which is modified, and not the crystallinity nor the crystal phase, as confirmed by the absence of significant broadening of the Bragg reflections in the X-ray diffraction (XRD) profiles. No anatase to rutile transformation was detected within the sensitivity of conventional X-ray diffraction. We note that this contrasts with the complete conversion observed by Criado and Real at similar rotation speed and grinding time [24]. We infer that this difference arises from the presence of the ZnO matrix which acts as a dispersant thus limiting the particle packing and decreasing the rate of phase transformation [25].

The second experiment consisted in a comparative study with a Degussa P25 $TiO_2$ powder. This powder is formed of aggregates of nanoparticles of about 25 nm in diameter mainly crystallized (80% anatase, 15% rutile, 5% amorphous).

Dispersions of the calcined Millennium and Degussa powders obtained after grinding were analyzed by dynamic light scattering, revealing comparable hydrodynamic diameter of ca. 120 nm (Fig. 4, left). This should be compared to the 50 nm diameter found for the commercial Millenium colloid. Films with similar $TiO_2$ content, thickness and porosity were prepared with the three kinds of particles, i.e. Millennium colloid and ground powder, and Degussa P25 ground powder. Due to the larger particle size, the films synthesized from the ground powders were slightly more diffusive than the reference one. Their photocatalytic activities were then evaluated by monitoring the degradation of the Rhodamine 6G dye deposited onto the surface of the films (Fig. 4, right).

The degradation curves are very similar for the three samples and fit to a first apparent order. Kinetics constants of $14 \times 10^{-3}$, $11 \times 10^{-3}$ and $18 \times 10^{-3}$ $min^{-1}$ were found for the Millennium colloid, the Millennium calcined powder and the Degussa P25 nanopowder, respectively. The main result is that these values are very similar, indicating (i) no decrease in photoactivity resulting from the grinding process that could induce a contamination by Zn or a partial amorphization as detected at higher energy milling [23] (comparison of the Millennium samples), (ii) the difference in size (120 nm instead of 50 nm) does not significantly affect the degradation rate and (iii) the Degussa P25 powder only exhibits a slightly improved degradation rate as compared to the Millennium samples [26].

But the most important conclusion deduced from these experiments is that the microstructure of the particles themselves only slightly affects the efficiency of the degradation process, probably because microstructure effects are mostly determined by the silica host matrix which is the same for all the three samples. This validates the method thus allowing a correct evaluation of the photocatalytic activity without artifact related to the initial morphology of the tested materials and an easy screening of new photocatalyst materials.

### 3.3. *N-doped $TiO_2$ nanoparticles*

According to the work of Asahi et al. [27] followed by many others, N-doping of $TiO_2$ still appears a promising strategy for the development of photocatalytic coatings active under visible light. Nitridation of $TiO_2$ is generally achieved through thermal treatment (from 600 to 1000 °C) with a nitrogen source. It is thus a case for which direct synthesis through colloidal routes is not possible and it is thus a case for which the grinding strategy previously described may be of interest. Nevertheless, we specifically developed another original route permitting thermal annealing of pristine anatase $TiO_2$ NPs up to 1000 °C without structural change, aggregation and growth of the particles [11] (Fig. 5).

In a first step of the doping procedure, pristine anatase $TiO_2$ NPs were dispersed in a sol–gel silica matrix using a copolymer template (BASF PE6800) to control the silica mesoporosity. After drying the sol, a white $TiO_2/SiO_2$ nanocomposite powder was obtained which was nitridated at different temperatures, using urea as the nitrogen source. XRD analysis indicates that these powders all present the anatase type structure after heating up to 800 °C.

$TiO_2/SiO_2$ nanocomposite powders obtained after nitridation exhibit a strong color from yellow to dark green (Fig. 6). The samples nitridated below 700 °C reflect the light essentially in the yellow, ranging for yellowish white to orange brown at 650 °C. Upon nitridation above 650 °C, the color suddenly turned dark green. This evolution, as observed to the eye, was confirmed by optical absorption measurements.

For the yellow powder nitridated at 500 °C, the absorption range is extended up to 550 nm as previously explained by the presence of localized N 2p states above the valence band maximum of $TiO_2$ [28]. The two types of N-based paramagnetic species, previously observed by Livraghi et al. [29,30], were detected by EPR on the yellow powder after nitridation at 600 °C. The EPR signal of the first type, noted $N_{ads.}$ (ads. = adsorbed) is characteristic of the adsorption of nitric oxide molecules (NO) at the surface

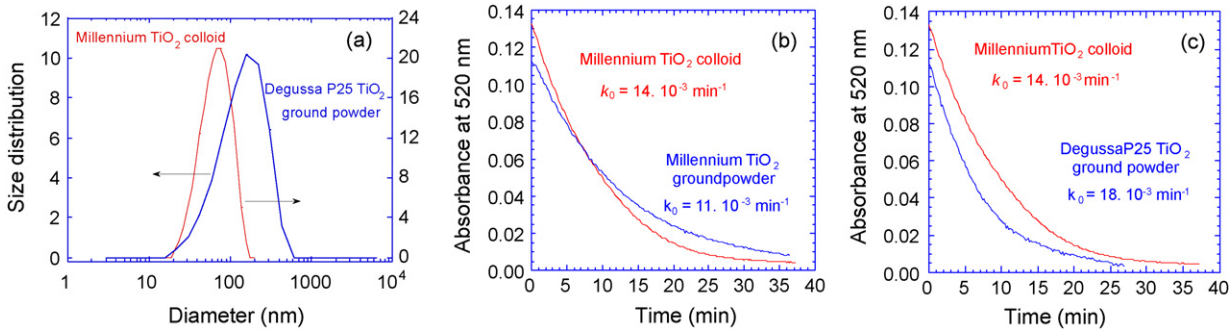


**Fig. 4.** (a) Size distribution obtained by dynamic light scattering on a commercial Millennium S5-300A $TiO_2$ colloid or from the same material dried at 90 °C, heated up to 450 °C for 2 h and then ground by ball milling. Kinetics of degradation of the Rhodamine 6G dye under UV irradiation (at 365 nm) measured on layers containing a same $TiO_2$ loading synthesized: (a) from the commercial Millennium $TiO_2$ colloid or from the same material dried at 90 °C, then heated up to 450 °C, 2 h and ground by ball milling; (b) from the commercial Millennium $TiO_2$ colloid or from a Degussa P25 $TiO_2$ powder dried at 90 °C and ground by ball milling. The typical error on $k_0$ is estimated to be 10%.

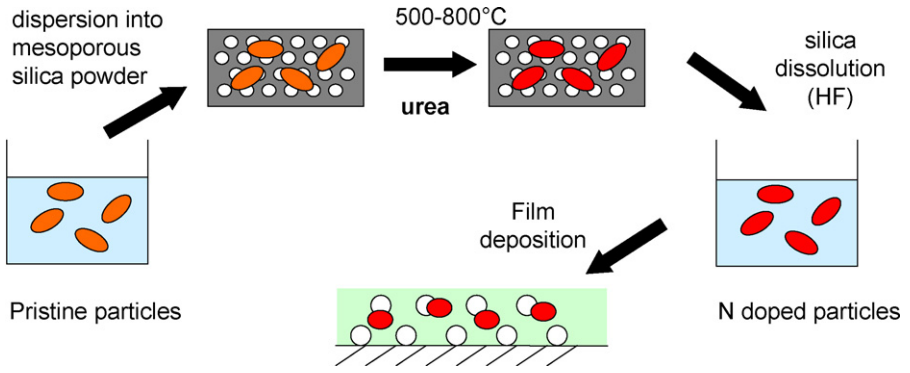


**Fig. 5.** Schematic presentation of the experimental procedure for the nitridation of $TiO_2$ NPs.

of different oxides. The second paramagnetic center, noted $N_{cryst.}$ (cryst. = crystal), was assigned to species containing a single nitrogen atom trapped into the structure of $TiO_2$. These $N_{cryst.}$ species have been proposed as responsible for the visible light sensitization of $TiO_2$ [30–32].

A striking feature is the sudden change of color from yellow-brown to dark green upon heating above 650 °C. Above this temperature, the atmosphere in the furnace is reductive, due to the partial decomposition of ammonia, and samples appear to be oxygen deficient. The green coloration is then essentially due to the presence of $Ti^{3+}$ ions adding a blue component to the yellow one. As shown by the absorption of the sample heated at 700 °C that covers all the visible range, the dark contribution could arise from minor phases such as TiN and/or titanium sub-oxides.

In a second step, $TiO_2/SiO_2$ nanocomposite powders were treated at room temperature by a diluted aqueous solution of hydrofluoric acid (HF 2 wt%) to dissolve the silica matrix. Under our experimental conditions, elemental analysis shows that silica was completely dissolved without significant alteration or fluorination of the $TiO_2$ NPs. After purification by centrifugation to remove the excess of hydrofluoric acid, the N-doped $TiO_2$ NPs powder was dispersed in an acidic aqueous medium (pH 1.25). This led to a wide range of colloidal aqueous suspensions of N-doped $TiO_2$ NPs (up to 50 g $L^{-1}$) obtained from $TiO_2/SiO_2$ nanocomposite powders nitridated from 550 to 800 °C.

The nitrogen doping level of the N-doped $TiO_2$ NPs in aqueous suspensions was quantified by elemental analysis. As the nitridation temperature increases up to 650 °C, the doping level progressively decreases. This could be explained by the temperature evolution of the adsorption/desorption equilibrium for the nitrogen species at the NPs surface. As expected, the doping level drastically increases above 650 °C, as the reducing atmosphere facilitates the nitrogen doping due to the formation of oxygen vacancies. Fig. 6 (right) schematically summarizes the qualitative evolution of doping species as a function of the nitridation temperature. $N_{ads.}$ species are first formed and their concentration progressively decreases in nanocomposites up to 650 °C while the concentrations of $N_{cryst.}$ and $Ti^{3+}$ species show a steep increase

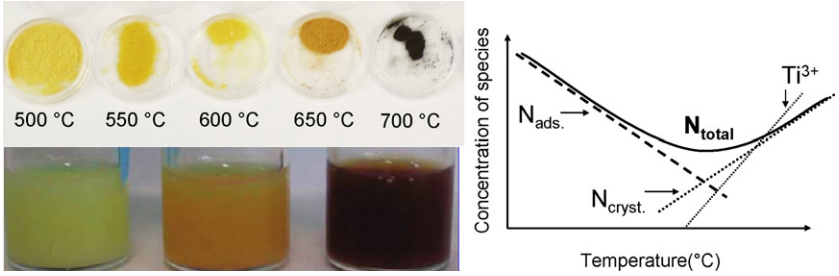


**Fig. 6.** Picture of the samples after nitridation within the silica matrix (top left), and after silica dissolution and recovery as colloidal suspension (bottom left). Schematic evolution of the defect concentration in N-doped $TiO_2$ NPs as a function of the nitridation temperature (right).

**Table 1**
Values of the $k_0$ constant corresponding to pseudo zero-order rate for kinetics curves. These values characterize the photocatalytic activity of mesoporous films with the same loading of pristine (TF-P) or N-doped $TiO_2$ NPs nitridated at temperatures ranging from 500 to 700 °C (TF-N500, TF-N600, TF-N700).

| $k_0$ ($10^{-4}$ min$^{-1}$) | TF-P | TF-N500 | TF-N600 | TF-N700 |
|---|---|---|---|---|
| UV | 19 | 11 | 9 | 10 |
| 390 nm | 0.21 | 0.24 | 0.85 | 4.90 |

above 650 °C due to the reductive atmosphere and formation of oxygen vacancies.

In a last step, aqueous suspensions of N-doped $TiO_2$ NPs were mixed in a copolymer/silica sol. Sol–gel thin films (400 nm in thickness) were deposited on glass substrates using the usual spin-coating technique. Films were then dried and heated in air at 450 °C first to remove the templating copolymer leading to films in which the N-doped $TiO_2$ NPs are dispersed in an organized mesoporous silica binder. Note that, contrasting with the corresponding NPs powders, no visible light absorption was detected on UV–vis spectra performed on these N-doped films, as expected from the weak amount of NPs per surface unit (4.6 μg cm$^{-2}$ of $TiO_2$ for all films). Moreover, it has been shown from thermal analysis experiments that a thermal treatment of N-doped $TiO_2$ NPs in air and above 300 °C, leads to samples with virtually no $Ti^{3+}$ but with a significant concentration of $N_{cryst.}$ species (>1 at.%). Therefore, the oxidative post-treatment of films at 450 °C allows suppressing $Ti^{3+}$ ions which are well known to act as recombination centers for the photoinduced electrons and holes, leading to a decreased photocatalytic activity [32,33].

The photoactivities of these films were evaluated by monitoring the decomposition of Rhodamine 6G. The dye was diluted in ethanol ($1.5 \times 10^{-3}$ mol L$^{-1}$) and spin-coated on the sample (2000 rpm, 60 s). The layer was irradiated under UV-A black-light or UV-LED (peak wavelength at 390 nm) while the absorption of Rhodamine 6G at 520 nm was monitored in situ. The determination of $k_0$ kinetic constants allows a quantitative comparison of the activity of the different films (Table 1).

Under excitation at 390 nm, the degradation of the TF-N700 mesoporous film is increased by a factor 20 compared to the TF-P one, giving a clear evidence of the influence of the N-doping on the degradation efficiency. The activity order for the films (TF-N700 > TF-N600 > TF-N500 > TF-P) appears as directly correlated to the concentration of $N_{cryst.}$ species which increases with the nitridation temperature of the NPs [34,35]. A previously proposed explanation is that the excited electrons from the N 2p levels near the valence band combine with adsorbed oxygen molecules to form catalytic species such as superoxide anions [28].

However, under UV irradiation, N-doped films exhibit lower photocatalytic activity than the TF-P films. In this case, the electrons both in the valence band and in the N 2p levels are excited to the conduction band. However, as reported by Tafen et al. [36], holes in the N 2p states are highly localized with a very low mobility and could act as recombination centers for the photogenerated charge carriers from the valence band.

## 4. Conclusions

This paper makes a brief review on our work toward the development of $TiO_2$-based thin films for the application of self-cleaning windows. The strategy that we have been exploring is the elaboration of thin films consisting in the dispersion of preformed colloidal $TiO_2$ particles within surfactant-templated mesoporous silica film. First aspect of our research concerns the investigation of the influence of the specific microstructure of these films in relation with their remarkable efficiency. The main conclusion is that the porosity allows the diffusion of the pollutant molecules within the whole film thickness, thus minimizing the required diffusion length of the reactive radicals generated at the particles surface. Second aspect of our studies concerns the investigation of the nature of the $TiO_2$ particles on the film efficiency. Application of an original grinding process allows studying different materials initially available as powders obtained through high temperature solid state reactions. The comparison between standard colloidal particles with grounded Degussa P25 $TiO_2$ nanopowder show similar efficiency. This validates the approach and shows that microstructure effects are mainly determined by the structure of the host silica binder. This surely opens the way toward the investigation of many other compounds with varying composition. Last part of our work concerns the investigation of N-doped particles for visible light activation. An original process has been developed which enables the nitridation of colloidal suspensions of $TiO_2$ particles while preserving their size and dispersion state. Characterization of the obtained materials evidences an effective visible light activation due to nitrogen insertion, although limited by a concomitant detrimental reduction of part of the $Ti^{4+}$. The latter effect may nevertheless be somewhat reduced through a post annealing treatment under air. Finally, it should be noted that if the nitrogen doping strategy is an efficient way for visible light sensitization, its application in self-cleaning transparent devices appears strongly limited due to a very limited absorbance of the films. This parameter, which strongly differentiates our targeted application as compared to others involving powders, evidences the importance of taking into account the absorption cross-section of materials when discussing of their application for self-cleaning windows.

## Acknowledgments

The authors wish to thank Sandrine Clary-Lespinasse for her kind help in the experiments. JPB and TGA wish to acknowledge the contribution of Sophie Besson at the beginning of the project. Part of this work was funded by the Saint-Gobain Company.

## References

[1] A. Mills, S. Le Hunte, An overview of semiconductor photocatalysis, J. Photochem. Photobiol. A 108 (1997) 1–35.
[2] J.D. DeLoach, G. Scarel, C.R. Aita, Correlation between titania film structure and near ultraviolet optical absorption, J. Appl. Phys. 85 (1999) 2377.
[3] A. Mills, N. Elliott, I.P. Parkin, S.A. O'Neill, R.J. Clark, Novel $TiO_2$ CVD films for semiconductor photocatalysis, J. Photochem. Photobiol. A: Chem. 151 (2002) 171.
[4] N. Negishi, T. Iyoda, K. Hashimoto, A. Fujishima, Preparation of transparent $TiO_2$ thin films photocatalyst and its photocatalytic activity, Chem. Lett. 9 (1995) 841.
[5] A. Mills, G. Hill, S. Bhopal, I.P. Parkin, S.A. O'Neill, Thick titanium dioxide films for semiconductor photocatalysis, J. Photochem. Photobiol. A: Chem. 160 (2003) 185.
[6] Y. Chen, S. Lunsford, D. Dionysios, Dionysiou, Photocatalytic activity and electrochemical response of titania film with macro/mesoporous texture, Thin Solid Films 516 (2008) 7930–7936.
[7] S. Besson, T. Gacoin, C. Ricolleau, C. Jacquiod, J.P. Boilot, Highly ordered orthorhombic mesoporous silica films, J. Mater. Chem. 13 (2003) 404.
[8] S.Y. Choi, M. Mamak, N. Coombs, N. Chopra, G.A. Ozin, Thermally stable two-dimensional hexagonal mesoporous nanocrystalline anatase, meso-nc-$TiO_2$: bulk and crack-free thin film morphologies, Adv. Funct. Mater. 14 (2004) 335.
[9] E.P. Reddy, B. Sun, P.G. Smirniotis, Transition metal modified $TiO_2$-loaded MCM-41 catalysts for visible- and UV-light driven photodegradation of aqueous organic pollutants, J. Phys. Chem. B 108 (2004), 17 198.
[10] E. Allain, S. Besson, C. Durand, M. Moreau, T. Gacoin, J.-P. Boilot, Transparent mesoporous nanocomposite films for self-cleaning applications, Adv. Funct. Mater. 17 (2007) 549.
[11] G. Mialon, M. Gohin, T. Gacoin, J.-P. Boilot, High temperature strategy for oxide nanoparticle synthesis, ACS Nano 2 (2008) 2505–2512.
[12] M. Gohin, I. Maurin, T. Gacoin, J.-P. Boilot, Photocatalytic activity of mesoporous films based on N-doped $TiO_2$ nanoparticles, J. Mat. Chem., in press.
[13] V. Roméas, P. Pichat, C. Guillard, T. Chopin, C. Lehaut, Degradation of palmitic (hexadecanoic) acid deposited on $TiO_2$-coated self-cleaning glass: kinetics of disappearance, intermediate products and degradation pathways, New J. Chem. 23 (1999) 365–373.

[14] D. Fattakhova-Rohlfing, J.M. Szeifert, Q. Yu, Vit Kalousek, J. Rathouský, T. Bein, Low-temperature synthesis of mesoporous titania-silica films with pre-formed anatase nanocrystals, Chem. Mater. 21 (2009) 2410–2417.
[15] J. Yin, Z. Zou, J. Ye, Possible role of lattice dynamics in the photocatalytic activity of $BaM_{1/3}N_{2/3}O_3$ (M = Ni, Zn; N = Nb, Ta), J. Phys. Chem. B 108 (2004) 8888–8893.
[16] Zou, J. Ye, K. Sayama, H. Arakawa, Photocatalytic hydrogen and oxygen formation under visible light irradiation with M-doped $InTaO_4$ (M = Mn, Fe, Co, Ni and Cu) photocatalysts, J. Photochem. Photobiol. A 148 (2002) 65–69.
[17] C. He, M. Gu, Photocatalytic activity of bismuth germanate $Bi_{12}GeO_{20}$ powders, Scripta Mater. 54 (2006) 1221–1225.
[18] L. Ge, M. Xu, H. Fang, Synthesis of novel photocatalytic $InVO_4$–$TiO_2$ thin films with visible light photoactivity, Mater. Lett. 61 (2007) 63–66.
[19] H. Zhang, X. Wu, Y. Wang, X. Chen, Z. Li, T. Yu, J. Ye, Z. Zou, Preparation of $Fe_2O_3$/$SrTiO_3$ composite powders and their photocatalytic properties, J. Phys. Chem. Solids 68 (2007) 280–283.
[20] R. Janot, D. Guérard, One-step synthesis of maghemite nanometric powders by ball-milling, J. Alloys Compd. 333 (2002) 302–307.
[21] J. Naser, W. Riehemann, H. Ferkel, Dispersion hardening of metals by nanoscaled ceramic powders, Mater. Sci. Eng. A 234–236 (1997) 467–469.
[22] M.V. Zdujić, O.B. Milošević, L.Č. Karanović, Mechanochemical treatment of ZnO and $Al_2O_3$ powders by ball milling, Mater. Lett. 13 (1992) 125–129.
[23] S. Bégin-Colin, A. Gadalla, G. Le Caër, O. Humbert, F. Thomas, O. Barres, F. Villiéras, L.F. Toma, G. Bertrand, O. Zahraa, M. Gallart, B. Hönerlage, P. Gilliot, On the origin of the decay of the photocatalytic activity of $TiO_2$ powders ground at high energy, J. Phys. Chem. C 113 (2009) 16589–16602.
[24] J. Criado, C. Real, Mechanism of the inhibiting effect of phosphate on the anatase → rutile transformation induced by thermal and mechanical treatment of $TiO_2$, J. Chem. Soc., Faraday Trans. 1 79 (1983) 2765–2771.
[25] S. Winardi, R.R. Mukti, K.-N.P. Kumar, J. Wang, W. Wunderlich, T. Okubo, Critical nuclei size, initial particle size and packing effect on the phase stability of sol-peptization-gel-derived nanostructured titania, Langmuir 26 (2010) 4567–4571 (and references therein).
[26] T. Ohno, K. Tokieda, S. Higashida, M. Matsumura, Synergism between rutile and anatase $TiO_2$ particles in photocatalytic oxidation of naphthalene, Appl. Catal. A 244 (2003) 383–391.
[27] R. Asahi, T. Morikawa, T. Ohwaki, K. Aoki, Y. Taga, Visible-light photocatalysis in nitrogen-doped titanium oxides, Science 293 (2001) 269–271.
[28] J. Wang, D.N. Tafen, J.P. Lewis, Z. Hong, A. Manivannan, M. Zhi, M. Li, N. Wu, Origin of photocatalytic activity of nitrogen-doped $TiO_2$ nanobelts, J. Am. Chem. Soc. 131 (2009) 12290–12297.
[29] S. Livraghi, A. Votta, M.C. Paganini, E. Giamello, The nature of paramagnetic species in nitrogen doped $TiO_2$ active in visible light photocatalysis, Chem. Commun. 4 (2005) 498–500.
[30] S. Livraghi, M.C. Paganini, E. Giamello, A. Selloni, C. Di Valentin, G. Pacchioni, Origin of photoactivity of nitrogen-doped titanium dioxide under visible light, J. Am. Chem. Soc. 128 (2006) 15666–15671.
[31] S. Livraghi, M.R. Chierotti, E. Giamello, G. Magnacca, M.C. Paganini, G. Cappelletti, C.L. Bianchi, Nitrogen-doped titanium dioxide active in photocatalytic reactions with visible light: multi-technique characterization of differently prepared materials, J. Phys. Chem. C 112 (2008) 17244–17252.
[32] N.J. Serpone, Is the band gap of pristine $TiO_2$ narrowed by anion- and cation-doping of titanium dioxide in second-generation photocatalysts? J. Phys. Chem. B 110 (2006) 24287–24293.
[33] S. Ikeda, N. Sugiyama, S. Murakami, H. Kominami, Y. Kera, H. Noguchi, K. Uosaki, T. Torimoto, B. Ohtani, Quantitative analysis of defectives sites in titanium (IV) oxide photocatalyst powders, Phys. Chem. Chem. Phys. 5 (2003) 778–783.
[34] Y. Nosaka, M. Matsushita, J. Nishino, A.Y. Nosaka, Nitrogen-doped titanium dioxide photocatalysts for visible response prepared by using organic compounds, Sci. Technol. Adv. Mater. 6 (2005) 143–148.
[35] Y. Wang, C. Feng, Z. Jin, J. Zhang, J. Yang, S. Zhang, A novel N-doped $TiO_2$ with high visible light photocatalytic activity, J. Mol. Catal. A: Chem. 260 (2006) 1–3.
[36] D.N. Tafen, J. Wang, N.Q. Wu, J.P. Lewis, Visible light photocatalytic activity in nitrogen-doped $TiO_2$ nanobelts, Appl. Phys. Lett. 94 (2009) 093101–093103.